Interface-Specific Vibrational Spectroscopy of Molecules with Visible Lights

Satoru Fujiyoshi,[†] Taka-aki Ishibashi,*[,‡] and Hiroshi Onishi[†]

Surface Chemistry Laboratory, Kanagawa Academy of Science and Technology (KAST), KSP East 308, 3-2-1 Sakado, Takatsu, Kawasaki, 213-0012, Japan, and Core Research for Evolutional Science and Technology, Japan Science and Technology Agency, 4-1-8 Honmachi, Kawaguchi, 332-0012, Japan

Received: May 17, 2004; In Final Form: June 16, 2004

Interface-specific observation of molecular vibrations was achieved with visible light by a fourth-order optical process. An aqueous solution of oxazine dye interfaced with air was irradiated with 16-fs pulses at 600 nm. A pump pulse excited Raman-active nuclear motions of the dye. A probe pulse interacted with the excited molecules to generate second harmonic light, the intensity of which was oscillated as a function of the pump−probe delay. Fourier transformation of the oscillation provided a vibrational spectrum of 0−1000 cm^{-1} for the dye located at the air−solution interface.

1. Introduction

There is a strong need to determine the chemical composition and molecular structure of various interfaces working in nature and in artificial devices.[1] Sum-frequency (SF) generation,[2−8] a second-order nonlinear optical process, is now widely used for this purpose. SF light is generated specifically at an interface irradiated with infrared (IR) and visible lights. A nonlinear optical process based on an even-order susceptibility $\chi^{(2n)}$ (n = 1, 2, ...) is forbidden in centrosymmetric media (bulk vapors, bulk liquids, and most bulk solids).[9] The intensity of the SF light as a function of the IR wavenumber provides a vibrational spectrum of molecules at the interfaces, since the efficiency of the SF process is enhanced by the vibrational resonance of the IR light. This successful method, however, possesses two major limitations. (1) Low transparency of IR light is problematic when observing interfaces buried in solids or in liquids, especially water. (2) It is still difficult to obtain an intense, low-frequency (<1000 cm^{-1}) IR light by using an advanced tabletop laser source. These difficulties have been partially fixed by experimental developments. A limited number of liquid−solid[6] and liquid−liquid[7] interfaces were probed with a total-reflection method. Vibrations below 1000 cm^{-1} were observed with the aid of a free-electron laser facility.[10]

In the present paper, we propose a more general solution: a time-domain spectroscopy based on fourth-order Raman scattering in which vibrational coherences are pumped by a Raman process (Figure 1a). A target interface is irradiated with a femtosecond pump pulse of a frequency (Ω). When the bandwidth of the pump pulse, typically 920 cm^{-1} for a 16-fs pulse duration, is broader than the energy difference between the ground (g) state and vibrational excited (v) states, the pulse coherently excites Raman-active modes of vibration (v ← e_1 ← g).[11] The energy of the pump light should be resonant with an electronic transition of the molecule (e_1 ← g) to enhance the efficiency of the Raman pumping. At a time delay of t_d, the probe light of the frequency Ω interacts with the coherently excited molecules to generate the signal light of the second harmonic frequency (2Ω). This pump−probe process contains four incident electric fields, and thus the signal field E_{fourth} is proportional to a fourth-order response, $\chi^{(4)}$. The even-order optical process offers an interface-specific observation of molecular vibrations. As in the case of a time-domain Raman measurement,[11] the time-evolution of the fourth-order Raman scattering due to $\chi^{(4)}$ is presented as the sum of exponentially decaying, periodic oscillations as a function of t_d:

$$E_{fourth}(t_d) \propto \chi^{(4)}(t_d) \propto \sum_v A_v \cos(\omega_v t_d + \varphi_v) \exp(-t_d/T_v) \quad (1)$$

where A_v, ω_v, φ_v, and T_v are the amplitude, frequency, phase, and dephasing time of each vibrational mode. The optical response $\chi^{(4)}(t_d)$ is converted to the vibrational spectrum $\chi^{(4)}(\omega_v)$ via Fourier transformation.

Surface phonons of inorganic materials, GaAs[12−14] and Cs/Pt(111),[15,16] have been observed using this fourth-order process.[17] Their pump−probe light pulses were fixed in wavelength.

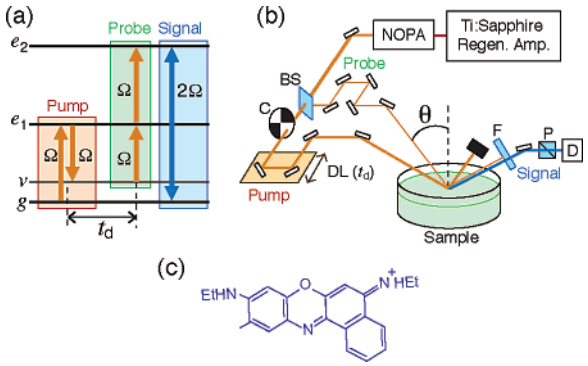

Figure 1. (a) Energy diagram of the fourth-order Raman process. The double-sided arrow indicates the fourth-order polarization at the frequency of 2Ω. (b) Schematic illustration of the spectrometer: BS, beam splitter; C, synchronous mechanical chopper; DL, optical delay line; θ, the angle between the probe light and surface normal; F, filter for the rejection of the probe light at the frequency Ω; P, Gran-Laser polarizing prism; D, detector. (c) Molecular structure of oxazine 170 dye.

* To whom correspondence should be addressed. E-mail: taib@hiroshima-u.ac.jp.

† Present address: Department of Chemistry, Faculty of Science, Kobe University, Nada, Kobe, 657-8501, Japan.

‡ Present address: Department of Chemistry, Graduate School of Science, Hiroshima University, Kagamiyama, Higashi-Hiroshima 739-8526, Japan.

10.1021/jp047877v CCC: $27.50
Published on Web 07/01/2004

We attempted in the present study to extend the observable objects by tuning the wavelength of the light pulses. The energy of the pump light should be resonant with an electronic transition at the interface ($e_1 \leftarrow g$) to enhance both the Raman-pump and probe efficiencies. A fourth-order Raman spectrometer tunable at 500−750 nm was constructed to achieve interface-specific, IR-free observation of molecular vibrations. This extended method might have wide applications.

2. Experimental Setup

Figure 1b shows a schematic illustration of our spectrometer with a reflection configuration. Pump (0.7 μJ) and probe (0.4 μJ) pulses were generated in a noncollinear optical parametric amplifier (TOPAS-*white*, Quantronix) pumped by a Ti:sapphire regenerative amplifier (Hurricane, Spectra Physics) operated at 1 kHz. The wavelength of the pulses was tunable within the range of 500−750 nm and tuned at 600 nm to be nearly resonant with the steady-state electronic absorption of oxazine 170 dye.[18] The *p*-polarized pump and *p*-polarized probe beams were focused and crossed on an oxazine solution interfaced air at the crossing angle of 2° with the incident angle $\theta \approx 65°$ for the probe. The *p*-polarized second-harmonic light was generated along the reflected direction and detected with a photomultiplier tube,[19] while the reflected probe light of the frequency Ω was blocked with a filter (F). The instrumental function and the time origin ($t_d = 0$ ps) were determined on the intensity cross-correlation of the pump and probe pulses using a second harmonic signal from a 50-μm-thick β-BaB_2O_4 crystal. The full width at half-maximum of the instrumental cross-correlation function (τ_{inst}) was 23 fs. Oxazine 170 (99%, Acros) was dissolved in HPLC-grade water (Wako) at a concentration of 0.2 mmol/L. The molecular structure of oxazine 170 is shown in Figure 1c. Sodium chloride (0.1 mol/L) was added to the solution to enhance the second harmonic intensity.[18]

3. Results and Discussion

The intensity of the second harmonic light, $I(2\Omega)$, of the oxazine 170 aqueous solution was plotted as a function of t_d (Figure 2a). It was instantaneously decreased at the pump excitation and fractionally recovered within several picoseconds. Periodic modulation superimposed on the nonoscillatory background reflects the vibrations of the dye at the interface. The whole intensity is given by

$$I(2\Omega) = |E_{SH}(t_d) + E_{fourth}(t_d)\exp(i\phi)|^2 \qquad (2)$$

with $E_{SH}(t_d) = E_0 + E_{Non}(t_d)$, where E_{fourth} denotes the electric field amplitude and ϕ represents the relative phase between E_{SH} and E_{fourth}. E_0 denotes the second harmonic light field generated at the unaffected (pump-free) interface, while $E_{Non}(t_d)$ is the pump-induced nonoscillatory modulation. With E_{fourth} much smaller than the others, which was the case in Figure 2a,

$$I(2\Omega) = |E_{SH}(t_d)|^2 + 2E_{fourth}(t_d)E_{SH}(t_d)\cos\phi \qquad (3)$$

and then the fourth-order Raman term is deduced as

$$E_{fourth}(t_d) \propto [I(2\Omega) - |E_{SH}(t_d)|^2]/E_{SH}(t_d) \qquad (4)$$

The nonoscillatory term, $E_{SH}(t_d)$, was estimated on a fitting analysis with multiexponential functions in the range of 0−5 ps.[20] The optimum fit was achieved with $\tau_1 < 23$ fs, $\tau_2 = 0.19$ ps, $\tau_3 = 2.6$ ps, and $\tau_4 > 5$ ps. The τ_3 and τ_4 components were

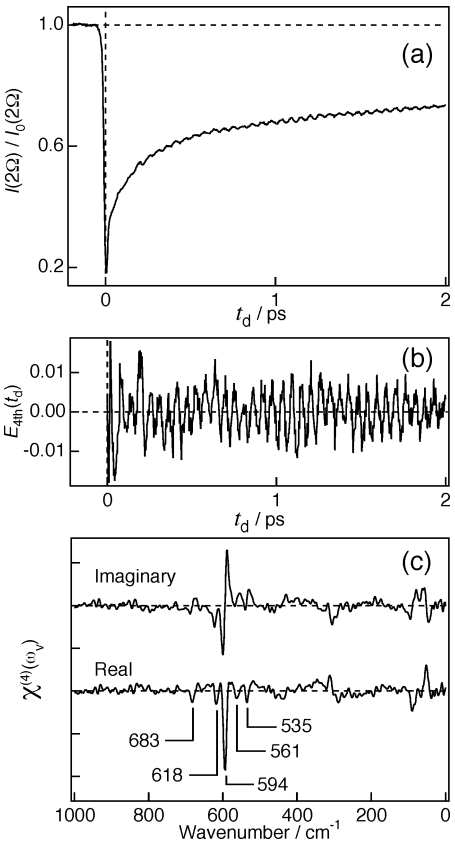

Figure 2. (a) Fourth-order Raman signal of oxazine 170 at the air−solution interface as a function of the time delay t_d. (b) Oscillated components deduced from (a). (c) Imaginary and real parts of the Fourier-transformed spectrum of the oscillation.

assigned by time-resolved second harmonic generation (TR-SHG) measurements[21] to the depletion of the dye molecules in the electronic ground state. The τ_1 and τ_2 components were assigned to an instantaneous electronic response[22,23] and the ultrafast solvation of the excited species,[24−27] respectively. The fourth-order Raman term estimated by eq 4 (Figure 2b) was Fourier-transformed to make a frequency-domain spectrum (Figure 2c).[28] Negative, symmetric-shape bands appeared at 535, 561, 594, 618, and 683 cm^{-1} in the real part of the Fourier-transformed spectrum, together with dispersive-shape bands at the corresponding wavenumbers in the imaginary part. Those bands were attributed to the dye molecules located at the air−solution interface because the observed oscillated second harmonic light was generated by the even-order (fourth-order) optical process.

Here we consider the transition probability of the fourth-order Raman scattering. This process consists of the pump and probe transitions. Raman-active vibrations are pumped with the aid of the resonance to the electronic excited state (e_1), whereas the probe process is equivalent to a hyper Raman process.[29] Hence, the cross section of the fourth-order Raman scattering is proportional to the product of a resonance Raman tensor (α) and a hyper Raman tensor (β).

To evaluate the Raman tensor (α), the resonance Raman spectrum of the bulk solution was observed with the spectrometer in Figure 1b. The time-dependent reflectance of the probe light was monitored instead of the 2Ω light. The time evolution of the reflectance change provides a time-domain representation of Raman-active vibrations of oxazine 170 in the solution.[30,31] Figure 3 shows the reflectance change,[32] its oscillatory component, and the Fourier-transformed spectrum of the oscillation

in a parallel manner with Figure 2. The real part of the Fourier-transformed spectrum corresponds to the spontaneous resonance Raman spectrum that is proportional to the square of the Raman tensor, $|\alpha|^2$.[33] Six bands at 294, 535, 560, 593, 619, and 682 cm^{-1} were identified in Figure 3c, five of which reproduced the center frequencies of the fourth-order Raman bands in Figure 2c. The band positions that are in agreement confirmed that the oscillated intensity of the second harmonic light represented the Raman-active modes of the dye. The agreement also suggests that the different dielectronic environments at the interface and in the solution caused a negligible shift of the vibrational wavenumbers. In contrast, the relative intensity of the 535-cm^{-1} and 560-cm^{-1} bands in Figure 2c was different from that of the corresponding bands in Figure 3c. The disagreement of the relative intensity is consistent with the predicted cross section containing the hyper-Raman tensor in addition to the Raman tensor, though the hyper-Raman spectrum of oxazine 170 has not been observed.

Finally, a possible contribution of an undesired optical process is considered and excluded. Two cascading independent third-order optical processes have sometimes been misidentified as a fifth-order process.[34] In our case, a pump-induced third-order process in the bulk solution is possibly coupled with the second harmonic generation at the interface to imitate the desired fourth-order Raman signal. The electric field generated by the third-order polarization pumped in the solution, $E_{\text{third}}(t_d)$, propagates to the interface and modulates the electric field of the incident probe light, E_{probe}. The intensity of the second harmonic light generated by the modulated probe field, $E_{\text{probe}}'(t_d)$, is

$$I(2\Omega) = |E_{\text{SH}}(t_d)|^2 \propto |\chi^{(2)}|^2 |E_{\text{probe}}'(t_d)|^4 = |\chi^{(2)}|^2 |E_{\text{probe}} + E_{\text{third}}(t_d) \exp(i\psi)|^4 \quad (5)$$

with ψ as the phase difference between the electric fields of E_{probe} and E_{third}. Assuming $|E_{\text{third}}| \ll |E_{\text{probe}}|$, the pump-induced change is approximated as

$$I(2\Omega)/I_0(2\Omega) \propto 1 + 4E_{\text{third}}(t_d) \cos\psi/E_{\text{probe}} \quad (6)$$

However, E_{third} at the interface is averaged to be virtually zero when integrated over the solution of a macroscopic dimension because of the phase-match requirement. Only the contribution of a thin solution layer of a thickness comparable with the probe-light wavelength is considered further. If the time-dependent transmittance of the solution layer is observable, the amplitude of the E_{third}-induced oscillation (ΔT) is given by

$$\Delta T = 2E_{\text{third}}(t_d) \cos\psi/E_{\text{probe}} \quad (7)$$

and thus

$$I(2\Omega)/I_0(2\Omega) \propto 1 + 2\Delta T \quad (8)$$

ΔT can be estimated on the amplitude of the reflectance oscillation (ΔR) of the interface as[30]

$$\Delta T/\Delta R = E_{\text{R0}}/E_{\text{probe}} \quad (9)$$

where E_{R0} denotes the reflected probe field. $|E_{\text{R0}}/E_{\text{probe}}|$ was 0.14 on our air−solution interface. $2|\Delta T|$ was thereby estimated to be 0.0001 on experimentally observed $|\Delta R| = 0.0005$ (Figure 3b). The oscillation amplitude of the second harmonic light in Figure 2a (~0.01) was larger by 2 orders of magnitude in comparison to the amplitude estimated on the cascaded $\chi^{(3)}$ and $\chi^{(2)}$ processes. The oscillated second harmonic light was therefore ascribed to the fourth-order Raman process.

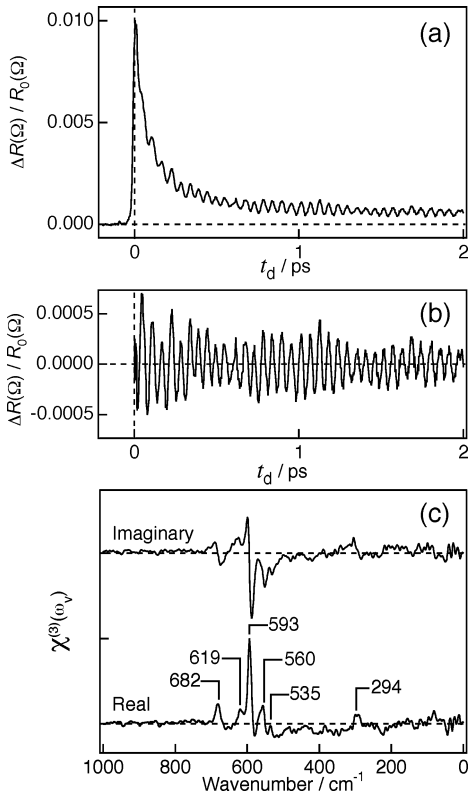

Figure 3. (a) Time-resolved reflectance change of the air−solution interface measured with the same pulse energies, polarizations, and incident angle as those of Figure 2. (b) Oscillated components deduced from a. (c) Imaginary and real parts of the Fourier-transformed spectrum of the oscillation.

In the present work, we have demonstrated fourth-order Raman spectroscopy, an interface-specific nonlinear vibrational spectroscopy. Molecular vibrations in the range of 0−1000 cm^{-1} were observable on an air−solution interface by using visible light pulses. This nonlinear optical method probing Raman-excited vibrations complements currently utilized sum-frequency spectroscopy of IR-excited vibrations at an interface. The application to an interface buried in a dense ambient and the extension of the low-wavenumber limit of detection are promising for this Raman-based method, in particular.

Acknowledgment. We thank R. Danielius (Light Conversion), M. Tatebayashi, T. Ohyama (Excel Technology), and T. Asai (Spectra Physics) for their help with the laser system. This work was supported by Grant-in-Aids for Scientific Research from the Ministry of Education, Culture, Sports, Science Technology of Japan (No. 14654108).

References and Notes

(1) Adams, D. M.; Brus, L.; Chidsey, C. E. D.; Creager, S.; Creutz, C.; Kagan, C. R.; Kamat, P. V.; Lieberman, M.; Lindsay, S.; Marcus, R. A.; Metzger, R. M.; Michel-Beyerle, M. E.; Millller, J. R.; Newton, M. D.; Rolison, D. R.; Sankey, O.; Schanze, K. S.; Yardley, J.; Zhu, X. *J. Phys. Chem. B* **2003**, *107*, 6668.

(2) Shen, Y. R. *Nature* **1989**, *337*, 519.

(3) Eisenthal, K. B. *Chem. Rev.* **1996**, *96*, 1343.

(4) Miranda, P. B.; Shen, Y. R. *J. Phys. Chem. B* **1999**, *103*, 3292.

(5) Roke, S.; Schins, J.; Müller, M.; Bonn, M. *Phys. Rev. Lett.* **2003**, *90*, 128101.

(6) Wang, J.; Even, M.; Chen, X.; Schmaier, A. H.; Waite, J. H.; Chen, Z. *J. Am. Chem. Soc.* **2003**, *125*, 9914.

(7) Scatena, L. F.; Brown, M. G.; Richmond, G. L. *Science* **2001**, *292*, 908.

(8) Ishibashi, T.; Onishi, H. *Appl. Phys. Lett.* **2002**, *81*, 1338.
(9) Shen, Y. R. *The Priciple of Nonlinear Optics*; Wiley-Interscience: New York, 1984.
(10) Braun, R.; Casson, B. D.; Bain, C. D.; van der Ham, E. W. M.; Vrehen, Q. H. F.; Eliel, E. R.; Brigg, A. M.; Davies, P. B. *J. Chem. Phys.* **1999**, *110*, 4634.
(11) Dhar, L.; Rogers, J. A.; Nelson, K. A. *Chem. Rev.* **1994**, *94*, 157.
(12) Chang, Y. M.; Xu, L.; Tom, H. W. K. *Phys. Rev. Lett.* **1997**, *78*, 4649.
(13) Tom, H. W. K.; Chang, Y. M.; Kwak, H. *Appl. Phys. B* **1999**, *68*, 305.
(14) Watanabe, K.; Dimitrov, D. T.; Takagi, N.; Matsumoto, Y. *Phys. Rev. B* **2002**, *65*, 235328.
(15) Watanabe, K.; Takagi, N.; Matsumoto, Y. *Chem. Phys, Lett.* **2002**, *366*, 606.
(16) Watanabe, K.; Takagi, N.; Matsumoto, Y. *Phys. Rev. Lett.* **2004**, *92*, 057401.
(17) The pump−probe method detecting 2Ω signal is regarded as time-resolved second harmonic generation (TR-SHG) technique. The oscillatory component due to $\chi^{(4)}$ is referred to as fourth-order Raman scattering, in an analogy with impulsive stimulated Raman scattering, an established time-domain spectroscopy based on $\chi^{(3)}$.
(18) Steinhurst, D. A.; Owrutsky, J. C. *J. Phys. Chem. B* **2001**, *105*, 3062.
(19) The output of the photomultiplier was gated with a boxcar integrator, A/D converted, and sent to the computer on a pulse-to-pulse basis. The pump pulse was modulated at 500 Hz with a synchronous mechanical chopper. The signals with pump-on and pump-off were separately accumulated, and the former was divided by the latter.
(20) The following functional form was assumed to fit $|E_{SH}(t_d)|^2$ at $t_d = -0.2-5$ ps: $F(t_d) = 1 + [a_1 \exp(-t_d/\tau_1) + a_2 \exp(-t_d/\tau_2) + a_3 \exp(-t_d/\tau_3) + a_4] \otimes \exp[4 \ln 2(-t_d/\tau_{inst})^2]$, where ⊗ means the convolution between the former and latter functions. τ_{inst} is the instrumental response time of the present measurement (23 fs).
(21) Steinhurst, D. A.; Baronavski, A. P.; Owrutsky, J. C. *J. Phys. Chem. B* **2002**, *106*, 3160.
(22) Ruhman, S.; Willliams, L. R.; Joly, A. G.; Kohler, B.; Nelson, K. A. *J. Phys. Chem.* **1987**, *91*, 2237.
(23) Fujiyoshi, S.; Takeuchi, S.; Tahara, T. *J. Phys. Chem. A* **2003**, *107*, 494.
(24) Meech, S. R.; Yoshihara, K. *Chem. Phys. Lett.* **1990**, *174*, 423.
(25) Zimdars, D.; Dadap, J. I.; Eisenthal, K. B.; Heinz, T. F. *Chem. Phys. Lett.* **1999**, *301*, 112.
(26) Benderskii, A. V.; Eisenthal, K. B. *J. Phys. Chem. B* **2001**, *104*, 11723.
(27) Shang, X.; Benderskii, A. V.; Eisenthal, K. B. *J. Phys. Chem. B* **2001**, *105*, 11578.
(28) Before the FT analysis, oscillations at 0−5 ps were multiplied with a window function (a Gaussian function of 4.5-ps full width at half-maximum), and zero data points were added at 5−25 ps to smooth the transformed spectrum.
(29) Long, D. A. *Raman Spectroscopy*; McGraw-Hill: New York, 1977.
(30) Fujiyoshi, S.; Ishibashi, T.; Onishi, H. *J. Phys. Chem. B* **2004**, *108*, 1525.
(31) Nagasawa, Y.; Watanabe, A.; Takikawa, H.; Okada, T. *J. Phys. Chem. A* **2003**, *107*, 632.
(32) The nonoscillatory background was well-fitted with three exponential functions convoluted with the instrumental response function (a Gaussian function having an fwhm of 23 fs) in the range of −0.3 to 5 ps. Time constants of $\tau_1 < 23$ fs, $\tau_2 = 0.11$ ps, $\tau_3 = 0.84$ ps, and $\tau_4 > 5$ ps were evaluated. The obtained time constants are different from those obtained from the second harmonic light. However, the time constants by the two methods cannot be directly compared with one another. In the reflection measurement, the amplitudes of the nonoscillatory components, $E_{non}(\Omega)$, were much smaller than that of the reflected probe light, $E_0(\Omega)$, so the observed reflectance change was linear to the nonoscillatory field, $E_{non}(\Omega)$. In contrast, the amplitudes of the nonoscillatory component, $E_{non}(2\Omega)$, of the second harmonic field was in the same order of $E_0(2\Omega)$. The homodyne signal, $|E_{non}(2\Omega)|^2$, contributes to the total signal as well as the heterodyne signal that was proportional to $E_{non}(2\Omega)$. Consequently, the time constants of the nonoscillatory components of the second harmonic light intensity were not directly related to the rate constants of the post-photoexcitation process of the dye.
(33) As in the case of $\chi^{(4)}(t_d)$ (eq 1), $\chi^{(3)}(t_d)$ (Figure 3c) provides four independent parameters: the amplitude A_v, the frequency ω_v, the dephasing time T_v, and the phase φ_v of a vibrational coherence. A_v, ω_v, and T_v correspond to the intensity, frequency, and bandwidth in the frequency-domain spontaneous Raman spectrum of the same sample. A band shape in the FT spectrum of $\chi^{(3)}(t_d)$ depends on φ_v. For example, when φ_v is equal to 0 ($\pi/2$), the coherence is expressed as an even (odd) function of t_d, the vibrational band in the real (imaginary) part is symmetric, and the band in its imaginary (real) part is dispersive. In contrast, the spontaneous Raman spectrum always has symmetric bands. All the observed bands of $\chi^{(3)}(\omega_v)$ having $\varphi_v = 0$, the symmetric bands in the real part correspond to the spontaneous Raman bands.
(34) Blank, D. A.; Kaufman, L. J.; Fleming, G. R. *J. Chem. Phys.* **1999**, *111*, 3105.
(35) Ziegler, L. D.; Fan, R.; Desrosiers, A. E.; Scherer, N. F. *J. Chem. Phys.* **1994**, *100*, 1823.